J. Fluid Mech. (1967), *vol.* 29, *part* 3, *pp.* 593–607
Printed in Great Britain

Solitary internal waves in deep water

By RUSS E. DAVIS† AND ANDREAS ACRIVOS
Department of Chemical Engineering, Stanford University

(Received 7 December 1966)

A new type of solitary wave motion in incompressible fluids of non-uniform density has been investigated experimentally and theoretically. If a fluid is stratified in such a manner that there are two layers of different density joined by a thin region in which the density varies continuously, this type of wave propagates along the density gradient region without change of shape. In contrast to previously known solitary waves, these disturbances can exist even if the fluid depth is infinite. The waves are described by an approximate solution of the inviscid equations of motion. The analysis, which is based on the assumption that the wavelength of the disturbance is large compared with the thickness, L, of the region in which the density is not constant, indicates that the propagation velocity, U, is characterized by the dimensionless group $(gL/U^2)\ln(\rho_1/\rho_2)$, where g is the gravitational acceleration and ρ is the density. The value of this group, which is dependent on the wave amplitude and the form of the density gradient, is of the order one. Experimentally determined propagation velocities and wave shapes serve to verify the theoretical model.

1. Introduction

Stably stratified fluids, when in motion, give rise to many fascinating phenomena which owe their existence to the interaction between density variations and gravity. One of the best known of these is the internal wave, presumably so named because, in contrast to more commonly encountered waves, it is formed deep within stratified fluids rather than on their surface. Although, admittedly, their effects may have been exaggerated at times—Pettersson (1912), for example, has suggested that such a seemingly non-maritime occurrence as the fall of the Roman empire may have been influenced by variations in internal tides—their importance in various geophysical problems cannot be discounted. For instance, naturally occurring internal waves may play a significant role in transport processes within oceans and estuaries, either directly by convection or indirectly by the generation of turbulence.

For the purposes of analysis, internal waves have been divided into two types: small-amplitude periodic waves and shallow water waves. In the former case (see Yih 1960*a*) the equations of motion are linearized by assuming that the wave amplitude is small compared to the wavelength, and the subsequent development yields an infinite number of modes of travelling periodic waves. On the other

† Present address: Institute of Geophysics and Planetary Physics, University of California, La Jolla.

hand, the analysis of shallow water internal waves, which has been discussed in detail by Benjamin (1966), is based on the simplifying assumption that the horizonal length scale of the motion is long compared with the fluid depth, and yields, in addition to periodic waves, an infinite number of travelling solitary wave modes.

The purpose of this paper is to present the results of a theoretical and experimental investigation of a new type of solitary internal wave which, in contrast to previously known solitary waves, can propagate in a fluid of infinite depth. To be more specific, it will be shown that in a stably stratified fluid consisting of two deep layers with constant densities ρ_1 and ρ_2 that are separated by a thin layer in which the density varies continuously, solitary waves can propagate down this thin layer with a characteristic wavelength much greater than the thickness of the region in which the density varies.† Thus, such waves are 'long waves' relative not to the depth of the fluid but rather to L, the thickness of the region of varying density.

In what follows we shall employ an inviscid analysis together with the Boussinesq approximation, thus reducing the basic equations to a relatively simple form for which approximate analytic solutions as well as a series of numerical solutions will be obtained. Although in principle an infinite number of modes of motion can exist, experimentally only the lowest of these has been observed and hence results will be presented only for that mode. These will indicate that the speed of propagation of the wave, U, is characterized by the dimensionless group $(gL/U^2)\ln(\rho_1/\rho_2)$, the value of which is dependent only on the form of the density gradient and the dimensionless amplitude of the wave. Wave propagation velocities are easily determined experimentally and, as will be shown, compare quite favourably with those predicted theoretically.

2. Analytic solutions

Although, physically, we consider here the unsteady flow associated with a wave propagating horizontally at constant velocity, $-U$, through a fluid which is quiescent at infinity, we can reduce the problem to one of steady motion by employing a co-ordinate system that moves with the wave. This allows us to use Long's (1953) integrated equation of motion for an incompressible, inviscid and non-diffusive fluid of variable density, which, in terms of dimensionless variables, is

$$\nabla^2\psi + \frac{d\ln\rho}{d\psi}\left[\frac{gL}{U^2}y + \tfrac{1}{2}(\psi_x^2+\psi_y^2)\right] = H(\psi),$$

where ψ is the dimensionless streamfunction and $H(\psi)$ is an arbitrary function of ψ. Here g denotes the gravitational constant, L is a characteristic length denoting the thickness of the non-uniform density layer and y is directed upwards. For the special case of uniform streaming at infinity H is simply

$$H(\psi) = \frac{d\ln\rho}{d\psi}\left[\frac{gL}{U^2}\psi + \tfrac{1}{2}\right],$$

† After completing this paper our attention was drawn to an independent and very detailed analytic study of this problem by T. Brooke Benjamin (1967), who showed that this type of wave can occur in various other stratified fluid configurations.

and the equation of motion becomes

$$\nabla^2\psi+\frac{d\ln\rho}{d\psi}\frac{gL}{U^2}(y-\psi)=\frac{1}{2}\frac{d\ln\rho}{d\psi}(1-\psi_x^2-\psi_y^2).$$

The subsequent development is based on the assumption that an approximate solution for weakly stratified fluids can be obtained by neglecting the right-hand side of this equation. Thus the basic equation becomes

$$\nabla^2\phi+\lambda\phi F(\phi+y)=0;\quad \phi\to 0\quad \text{as}\quad x^2+y^2\to\infty, \tag{1}$$

where $\phi=\psi-y$, $d\ln\rho/d\psi$ has been denoted as $(d\ln\rho/d\psi)_{\max}F(\psi)$ with $F\geqslant 0$, and $\lambda=-(gL/U^2)(d\ln\rho/d\psi)_{\max}$.

At this point, before proceeding with the discussion of deep water solitary internal waves, it is worth while to consider briefly their shallow water counterparts, i.e. to seek a solution of equation (1) which vanishes at $y=\pm 1$ and as $x\to\pm\infty$. This can best be accomplished by using the shallow water approximation in which the x-derivative of ϕ is assumed to be $O(\epsilon)$ smaller than the y-derivative, with $\epsilon\ll 1$. Consequently, (1) is written in terms of the stretched variable $\hat{x}=\epsilon x$, ϕ and λ are expanded in appropriate powers of ϵ as shown below:

$$\phi=\epsilon^2\phi^{(1)}+\epsilon^4\phi^{(2)}+\ldots,\quad \text{and}\quad \lambda=\lambda^{(0)}+\epsilon^2\lambda^{(1)}+\ldots,$$

while $F(\phi+y)$ is expanded into

$$F(\phi+y)=F(y)+F'(y)\phi+\ldots,$$

which is certainly permissible in view of the assumption that $\phi\ll 1$. In place of (1) we then obtain

$$\epsilon^2[\phi^{(1)}_{yy}+\lambda^{(0)}F(y)\phi^{(1)}]+\epsilon^4[\phi^{(2)}_{yy}+\lambda^{(0)}F(y)\phi^{(2)}+\lambda^{(1)}F(y)\phi^{(1)}+\lambda^{(0)}F'(y)(\phi^{(1)})^2+\phi^{(1)}_{\hat{x}\hat{x}}]+O(\epsilon^6)=0, \tag{2}$$

the $O(\epsilon^2)$ term of which is satisfied by setting $\phi^{(1)}=f(\hat{x})p(y)$, where

$$p''+\lambda^{(0)}F(y)p=0;\quad p(\pm 1)=0$$

and $f(\hat{x})$ is arbitrary. We wish to note here, in connexion with the deep water solitary wave solutions to be developed shortly, that, of the infinite number of eigenfunctions of this Sturm–Liouville system, the function $p(y)$ corresponding to the lowest mode has no zero in the interval $-1<y<1$.

With $\phi^{(1)}$ known, the $O(\epsilon^4)$ terms of (2) now yield a linear inhomogeneous equation for $\phi^{(2)}$ which has a solution only for particular forms of $f(\hat{x})$. To show this we express the solution of the $O(\epsilon^4)$ terms of (2) as

$$\phi^{(2)}=\lambda^{(1)}f(\hat{x})h_1(y)+f^2(\hat{x})h_2(y)+f''(\hat{x})h_3(y),$$

where h_1, h_2 and h_3 are solutions of the inhomogeneous equations

$$h_1''+\lambda^{(0)}Fh_1=-Fp,\quad h_2''+\lambda^{(0)}Fh_2=-F'p^2,\quad h_3''+\lambda^{(0)}Fh_3=-p,$$

satisfying the boundary conditions $h_1=h_2=h_3=0$ at $y=-1$. The second boundary condition, that $\phi^{(2)}=0$ at $y=1$, requires then that

$$f''+\lambda^{(1)}\frac{h_1(1)}{h_3(1)}f+\frac{h_2(1)}{h_3(1)}f^2=0,$$

which has the solution, corresponding to a solitary wave,

$$f = \operatorname{sech}^2\left[\hat{x}\left(\frac{h_2(1)}{6h_3(1)}\right)^{\frac{1}{2}}\right] \quad \text{and} \quad \lambda^{(1)} = -\frac{2}{3}\frac{h_2(1)}{h_1(1)}.$$

Long (1965) has pointed out that this analysis, which is based on an equation of motion that has been simplified according to the Boussinesq approximation, can lead to erroneous results if $F'(\psi)$ is small; nevertheless, it suffices to demonstrate the principal features of shallow water solitary internal waves.

We now turn our attention to fluids of infinite depth. To simplify the analysis we shall consider only two particular forms of the function $F(\psi)$ which, however, are representative of density configurations generally encountered in practice. In the first case, we shall set F equal to unity for $-1 < \psi < 1$ and equal to zero everywhere else, thus dividing up the fluid into three layers in which the equation of motion will be linear with, however, non-linear boundary conditions at the dividing streamlines. For our second problem we shall set $F(\psi) = \operatorname{sech}^2\psi$, and then attack equation (1) by the method of inner and outer expansions; this method could, of course, be applied equally well for any acceptable form of F, but the function $\operatorname{sech}^2\psi$ seems to be physically attainable as well as an adequate approximation of a class of density gradients that often occur naturally.

Let us consider the three-layer solution for which $F = 1$ for $-1 < \psi < 1$ and $F = 0$ elsewhere. In the various layers (1) becomes

$$\begin{aligned}
&\nabla^2\phi_1 = 0 \quad \text{for} \quad \psi \geqslant 1,\\
&\nabla^2\phi_2 + \lambda\phi_2 = 0 \quad \text{for} \quad -1 < \psi < 1,\\
&\nabla^2\phi_3 = 0 \quad \text{for} \quad \psi \leqslant -1.
\end{aligned}$$

At the dividing streamlines, $\psi = \pm 1$, well-known kinematic and dynamic conditions require that ψ and the pressure be continuous, which, as shown by Yih (1960*b*), also implies continuity of velocity in cases where the density is continuous. Hence, letting Y_1 and Y_3 be respectively the y co-ordinates of $\psi = 1$ and $\psi = -1$, we obtain the appropriate boundary conditions

$$\begin{aligned}
&\phi_1 = \phi_2, \quad \partial\phi_1/\partial y = \partial\phi_2/\partial y \quad \text{at} \quad y = Y_1 = 1 - \phi_1(x, Y_1),\\
&\phi_3 = \phi_2, \quad \partial\phi_3/\partial y = \partial\phi_2/\partial y \quad \text{at} \quad y = Y_3 = -1 - \phi_3(x, Y_3).
\end{aligned}$$

As was the case in the analysis of shallow water waves, we assume now that the waves we are describing are 'long' and introduce the stretched co-ordinate $\hat{x} = \epsilon x$ with $\epsilon \ll 1$. Also, in order to prevent the equations in layers 1 and 3 from degenerating completely, we stretch the y co-ordinates in layers 1 and 3 by means of $\hat{y} = \epsilon(y-1)$ and $\hat{y} = \epsilon(y+1)$. And, finally, we expand the principal dependent variables in the small parameter ϵ in the usual fashion:

$$\phi = \epsilon\phi^{(1)} + \epsilon^2\phi^{(2)} + \ldots, \quad \lambda = \lambda^{(0)} + \epsilon\lambda^{(1)} + \ldots,$$

which, in contrast to the expansion used for shallow water waves, assumes that the horizontal length scale is inversely proportional to the first power of the wave amplitude. Consequently, the equation of motion in layer 2 becomes

$$\epsilon\left[\frac{\partial^2\phi_2^{(1)}}{\partial y^2} + \lambda^{(0)}\phi_2^{(1)}\right] + \epsilon^2\left[\frac{\partial^2\phi_2^{(2)}}{\partial y^2} + \lambda^{(0)}\phi_2^{(2)} + \lambda^{(1)}\phi_2^{(1)}\right] + O(\epsilon^3) = 0, \tag{3}$$

while the equations in the other two layers remain unchanged. In addition, by expanding ϕ in a Taylor series about $y = 1$ and $y = -1$, we obtain

$$Y_1 = 1 - \epsilon\phi_2^{(1)}(\hat{x}, 1) + O(\epsilon^2), \quad Y_3 = -1 - \epsilon\phi_2^{(1)}(\hat{x}, -1) + O(\epsilon^2),$$

which, in turn, lead to the linearized boundary conditions at $y = 1$

$$\epsilon\phi_1^{(1)}(\hat{x}, 0) + \epsilon^2\phi_1^{(2)}(\hat{x}, 0) + O(\epsilon^3) = \epsilon\phi_2^{(1)}(\hat{x}, 1) + \epsilon^2\left[\phi_2^{(2)}(\hat{x}, 1) - \frac{\partial\phi_2^{(1)}}{\partial y}\bigg|_{y=1}\phi_2^{(1)}(\hat{x}, 1)\right] + O(\epsilon^3), \tag{4}$$

and

$$\epsilon^2\frac{\partial\phi_1^{(1)}}{\partial\hat{y}}\bigg|_{\hat{y}=0} + O(\epsilon^3) = \epsilon\frac{\partial\phi_2^{(1)}}{\partial y}\bigg|_{y=1} + \epsilon^2\left[\frac{\partial\phi_2^{(2)}}{\partial y}\bigg|_{y=1} - \frac{\partial^2\phi_2^{(1)}}{\partial y^2}\bigg|_{y=1}\phi_2^{(1)}(\hat{x}, 1)\right] + O(\epsilon^3), \tag{5}$$

together with a similar set resulting from the expansion about $y = -1$.

From inspection of the $O(\epsilon)$ terms of (3) and (5) we can readily see then that they admit the solutions

$$\phi_2^{(1)} = f(\hat{x})\begin{Bmatrix}\sin\frac{1}{2}(2n-1)\pi y\\ \cos n\pi y\end{Bmatrix}.$$

However, as mentioned earlier, only the lowest mode,

$$\phi_2^{(1)} = f(\hat{x})\sin\tfrac{1}{2}\pi y, \quad \lambda^{(0)} = \tfrac{1}{4}\pi^2,$$

will be considered here since it is the only one that has been observed experimentally. Also, since, in this case, ϕ is odd about $y = 0$ it suffices to consider the problem only in the upper half-plane.

On the other hand, inside the constant density layer,

$$\nabla^2\phi_1^{(1)} = 0; \quad \phi_1^{(1)} = f(\hat{x}) \quad \text{at} \quad \hat{y} = 0, \tag{6}$$

where the boundary condition at $\hat{y} = 0$ follows directly from the $O(\epsilon)$ terms of (4).

Returning now to the variable density layer, we see by inspection of the $O(\epsilon^2)$ terms of (3) that

$$\phi_2^{(2)} = (\lambda^{(1)}/\pi)f(\hat{x})\, y\cos(\tfrac{1}{2}\pi y),$$

where only the particular solution has been retained since addition of a multiple of the homogeneous solution, $\phi_2^{(1)}$, would simply be equivalent to a redefinition of the arbitrary constant ϵ. As a result, the $O(\epsilon^2)$ terms of (5) reduce to

$$\frac{\partial\phi_1^{(1)}}{\partial\hat{y}}\bigg|_{\hat{y}=0} = -\frac{\lambda^{(1)}}{2}f(\hat{x}) + \frac{\pi^2}{4}f^2(\hat{x}), \tag{7}$$

which constitutes a second boundary condition on the function $\phi_1^{(1)}$ of equation (6).

Before proceeding with the solution of (6) and (7) let us consider the case where $F = \operatorname{sech}^2\psi$. As in the three-layer solution, we let $\hat{x} = \epsilon x$ and expand ϕ and λ in powers of ϵ. Also, by virtue of the smoothness of the density gradient, we expand $F(\psi)$ in a Taylor series about $\psi = y$,

$$F(\psi) = \operatorname{sech}^2 y - 2\epsilon\operatorname{sech}^2 y\tanh y\phi^{(1)}(\hat{x}, y) + O(\epsilon^2),$$

which leads to

$$\epsilon\left[\frac{\partial^2\phi^{(1)}}{\partial y^2}+\lambda^{(0)}\operatorname{sech}^2 y\phi^{(1)}\right]$$
$$+\epsilon^2\left[\frac{\partial^2\phi^{(2)}}{\partial y^2}+\lambda^{(0)}\operatorname{sech}^2 y\phi^{(2)}+\lambda^{(1)}\operatorname{sech}^2 y\phi^{(1)}-2\lambda^{(0)}\operatorname{sech}^2 y\tanh y\phi^{(1)^2}\right]+O(\epsilon^3)=0 \tag{8}$$

in place of (1).

It is immediately apparent now from the $O(\epsilon)$ terms of this equation that there is no solution for $\phi^{(1)}$ which vanishes as y approaches infinity, implying a breakdown of the approximation scheme adopted here, due to the fact that, as $y\to\infty$, $\partial\phi^{(1)}/\partial y$ does not remain large compared with $\epsilon\,\partial\phi^{(1)}/\partial\hat{x}$. Hence the problem cannot be treated by a regular perturbation and must be approached instead via the method of inner and outer expansions. We consider, therefore, the domain of validity of (8) to be an 'inner' region and introduce an 'outer' region in which the appropriate co-ordinates are $(\hat{x},\hat{y})=(\epsilon x,\epsilon y)$ and ϕ is denoted by $\hat{\phi}$. On substituting this into (1) and noting the behaviour of $\operatorname{sech}^2(\hat{y}/\epsilon)$ as $\epsilon\to 0$, we obtain then the equation of motion in the outer region

$$\epsilon\nabla^2\hat{\phi}^{(1)}+\epsilon^2\nabla^2\hat{\phi}^{(2)}+O(\epsilon^3)=0,$$

together with the appropriate matching condition between the inner region and the outer region

$$\lim_{y\to\infty}\phi=\lim_{\hat{y}\to 0}\hat{\phi}.$$

Again, only the upper half-plane will be considered, since, as in the case of the three-layer solution, ϕ is odd about $y=0$. Also, owing to the analytic nature of $\hat{\phi}$ in the outer region, we may expand $\hat{\phi}(\hat{x},\hat{y})$ in a Taylor series about $\hat{y}=0$ yielding, for the matching requirement,

$$\lim_{y\to\infty}\phi=\epsilon\hat{\phi}^{(1)}(\hat{x},0)+\epsilon^2\left[\phi^{(2)}(\hat{x},0)+\left.\frac{\partial\phi^{(1)}}{\partial\hat{y}}\right|_{\hat{y}=0}y\right]+O(\epsilon^3).$$

Now, the lowest mode solution of the $O(\epsilon)$ part of (8) which remains finite as $y\to\infty$ is

$$\phi^{(1)}=f(\hat{x})\tanh y,\quad \lambda^{(0)}=2,$$

which matches, to $O(\epsilon)$, with $\hat{\phi}^{(1)}$ specified by

$$\nabla^2\hat{\phi}^{(1)}=0;\quad \hat{\phi}^{(1)}=f(\hat{x})\quad\text{at}\quad\hat{y}=0. \tag{9}$$

Similarly, the non-homogeneous solution of the $O(\epsilon^2)$ part of (8) becomes

$$\phi^{(2)}=-\tfrac{1}{3}\lambda^{(1)}f(\hat{x})\ln(\cosh y)\tanh y+f^2(\hat{x})\left[\tfrac{4}{5}\ln(\cosh y)\tanh y-\tfrac{2}{5}\tanh^3 y\right],$$

which has the limiting form, as $y\to\infty$,

$$\phi^{(2)}\sim-\tfrac{1}{3}\lambda^{(1)}f(\hat{x})(y+\ln\tfrac{1}{2})+f^2(\hat{x})(\tfrac{4}{5}y+\tfrac{4}{5}\ln\tfrac{1}{2}-\tfrac{2}{5}).$$

This, when inserted in the matching condition, yields for the 'outer' function $\phi^{(2)}$

$$\nabla^2\hat{\phi}^{(2)}=0;\quad \hat{\phi}^{(2)}=\tfrac{1}{3}\lambda^{(1)}\ln 2f(\hat{x})-(\tfrac{4}{5}\ln 2+\tfrac{2}{5})f(\hat{x})\quad\text{at}\quad\hat{y}=0,$$

as well as the following relation, which, along with equation (9), determines $f(\hat{x})$ and $\lambda^{(1)}$,

$$\left.\frac{\partial \hat{\phi}^{(1)}}{\partial \hat{y}}\right|_{\hat{y}=0} = -\frac{\lambda^{(1)}}{3} f(\hat{x}) + \tfrac{4}{5} f^2(\hat{x}). \tag{10}$$

Although, of course, a direct comparison between the 'layers' in the three-layer solution and the 'regions' in the inner and outer expansion method cannot be taken too literally, the similarity of the two solutions is marked. For one thing, the eigenfunctions have similar forms, each having a single zero, in contrast to the lowest solitary water internal wave mode, which, excluding the boundaries, has no zero. Furthermore, we find that in each case the unknown function $f(\hat{x})$, with $|f(0)| = 1$, and the first correction to λ must satisfy the system

$$\nabla^2 \phi = 0; \quad \phi = f(\hat{x}), \quad \partial\phi/\partial\hat{y} = -A\lambda^{(1)} f(\hat{x}) + B f^2(\hat{x}) \quad \text{at} \quad \hat{y} = 0,$$

where, for the three-layer method, $A = \frac{1}{2}$ and $B = \frac{1}{4}\pi^2$ (see equations (6) and (7)), while for the inner and outer solution $A = \frac{1}{3}$ and $B = \frac{4}{5}$ (see equations (9) and (10)), which can be reduced to the single form

$$\nabla^2 \tilde{\phi} = 0; \quad \tilde{\phi} = q(\tilde{x}) \quad \text{and} \quad \frac{\partial \tilde{\phi}}{\partial \tilde{y}} = q^2 - \frac{\lambda^{(1)}}{|\lambda^{(1)}|} q \quad \text{at} \quad \tilde{y} = 0 \tag{11}$$

by using the transformations

$$(\tilde{x}, \tilde{y}) = A\,|\lambda^{(1)}|\,(\hat{x}, \hat{y}) \quad (q(\tilde{x}), \tilde{\phi}) = \frac{B}{A\,|\lambda^{(1)}|}\,(f, \phi).$$

The solution to (11) is now (Courant & Hilbert 1953)

$$\tilde{\phi} = \frac{1}{\pi} \int_{-\infty}^{\infty} \frac{\tilde{y} q(\xi)}{(\tilde{x}-\xi)^2 + \tilde{y}^2} d\xi, \tag{12}$$

where, in view of the second boundary condition in (11), q must satisfy the non-linear integral equation

$$q^2(\tilde{x}) - \frac{\lambda^{(1)}}{|\lambda^{(1)}|} q(\tilde{x}) = \frac{1}{\pi} P \int_{-\infty}^{\infty} \frac{1}{\xi - \tilde{x}} \frac{dq}{d\xi} d\xi. \tag{13}$$

Equation (13) was solved at first numerically by a finite-difference technique, but, as shown by Benjamin (1967), it admits the exact solution

$$q(\tilde{x}) = -\frac{2}{1+\tilde{x}^2} \quad \text{with} \quad \lambda^{(1)} < 0,$$

which we subsequently found to be in excellent agreement with our numerical results. Hence, as shown also by Benjamin, the outer solution $\tilde{\phi}$ becomes simply

$$\tilde{\phi} = \frac{-2(1+\tilde{y})}{(1+\tilde{y})^2 + \tilde{x}^2}, \tag{14}$$

from which it is a simple matter to recover either $\phi^{(1)}$ of the three-layer solution or $\hat{\phi}^{(1)}$ of the inner and outer expansion solution, and thus to complete the first term of the solution to equation (1). The result of perhaps the greatest interest is that $\lambda^{(1)} = -\frac{1}{2}B/A$, which allows us to compute directly the rate at which the wave propagation velocity increases with increasing wave amplitude.

3. Numerical solutions

In order to extend the approximate analytic results of the previous section, which are valid only for small wave amplitudes, we present here the results of a study of the finite-difference equivalent of the equation of motion. It will be shown that, although this approach allows us to approximate the solution to (1) for arbitrarily large wave amplitudes, the equation itself becomes invalid for large waves whenever regions of closed streamline flow occur. Nevertheless, there is a considerable range of amplitudes for which the analytic results presented earlier are not adequate while valid numerical solutions can be found.

The introduction of the mesh dimensions δ_x, δ_y and the indices i, j defined by $x_i = (2i+1)\,\delta_x$, $y_j = 2j\delta_y$ allows us now to obtain the finite-difference form of (1),

$$\frac{\phi_i^{j+1}+\phi_i^{j-1}-2\phi_i^j}{(2\delta_y)^2}+\frac{\phi_{i+1}^j+\phi_{i-1}^j-2\phi_i^j}{(2\delta_x)^2}+\lambda\phi_i^j F(\phi_i^j+2j\delta_y)=0. \tag{15}$$

Although, in principle, these could be solved for an arbitrary choice of F, the required computation time would be extremely large owing to the large dimensions of the flow field and the need for a mesh size small enough to resolve the details of the flow. However, if we restrict ourselves to the three-layer model, $F = 1$ for $-1 < \phi_i^j + 2j\delta_y < 1$ and $F = 0$ otherwise, we can significantly reduce the computational difficulty by employing a rather novel technique based on the use of the finite difference equivalent of a Green's function, G_m^n, defined by

$$\frac{G_m^{n+1}+G_m^{n-1}-2G_m^n}{(2\delta_y)^2}+\frac{G_{m+1}^n+G_{m-1}^n-2G_m^n}{(2\delta_x)^2}=\begin{cases}-1 & \text{if} \quad n=m=0,\\ 0 & \text{if} \quad n\neq 0 \quad \text{or} \quad m\neq 0.\end{cases}$$

Clearly, the solution of this equation should approach a multiple of the fundamental solution of Laplace's equation, $\ln(r)$, as n and m tend to infinity provided that δ_x and δ_y are both small enough. Hence, it was decided to obtain G by solving this equation via a standard relaxation technique subject to the boundary condition that as n and m become large

$$G_n^m = C\ln([n\delta_x]^2+[m\delta_y]^2).$$

The value of C was adjusted so that the strength of the 'source' at $m = n = 0$ was -1.

Because the 'function' G behaves, in a sense, like the Green's function for Poisson's equation, it can be seen that (15) admits the solution

$$\phi_i^j = \sum_{\bar{i}=-\infty}^{\infty}\sum_{\bar{j}=-\infty}^{\infty} G_{i-\bar{i}}^{j-\bar{j}}\phi_{\bar{i}}^{\bar{j}}\lambda F(\phi_{\bar{i}}^{\bar{j}}+2\delta_y\bar{j}), \tag{16}$$

but, since $F = 0$ throughout most of the field, this may be reduced to the smaller system of linear equations

$$\frac{1}{\lambda}\phi_i^j = \sum_{\bar{i}=-\infty}^{\infty}\sum_{\bar{j}=-J(\bar{i})}^{J(\bar{i})} G_{i-\bar{i}}^{j-\bar{j}}\phi_{\bar{i}}^{\bar{j}},$$

where $J(\bar{i})$ is the largest j index for which $\phi_{\bar{i}}^{\bar{j}} + 2\delta_y\bar{j}$ is less than unity. By intro-

ducing the symmetry properties $\phi(x, -y) = -\phi(x, y)$ and $\phi(-x, y) = \phi(x, y)$ this simplifies to

$$\frac{1}{\lambda}\phi_i^j = \sum_{\bar{\imath}=0}^{\infty} \sum_{\bar{\jmath}=0}^{J(\bar{\imath})} K(i, j; \bar{\imath}, \bar{\jmath})\, \phi_{\bar{\imath}}^{\bar{\jmath}}, \tag{17}$$

with $$K(i, j; \bar{\imath}, \bar{\jmath}) = G_{i-\bar{\imath}}^{j-\bar{\jmath}} - G_{i-\bar{\imath}}^{j+\bar{\jmath}} + G_{i+\bar{\imath}+1}^{j-\bar{\jmath}} - G_{i+\bar{\imath}+1}^{j+\bar{\jmath}}.$$

Furthermore, noting that

$$K \to \ln\left(\frac{[j-\bar{\jmath}]^2 + [i-\bar{\imath}]^2}{[j+\bar{\jmath}]^2 + [i-\bar{\imath}]^2}\right)\left(\frac{[j-\bar{\jmath}]^2 + [i+\bar{\imath}+1]^2}{[j+\bar{\jmath}]^2 + [i+\bar{\imath}+1]^2}\right) \to 0$$

as $j/\bar{\jmath} \to \infty$, we see that since $0 \leqslant \bar{\jmath} \leqslant J$, the solution of equation (17) automatically vanishes as $y^2 \to \infty$. Hence we need require only that $\phi \to 0$ as $\bar{\imath} \to \infty$.

The solution of (17) is, of course, complicated by the fact that the location of the points $J(\bar{\imath})$ is not known in advance; but, since it is not difficult to estimate the shape of the dividing streamline $\psi = 1$, we can proceed as follows: (i) we choose a reasonable shape for the dividing streamline $\psi = 1$, thus locating approximately the points $J(\bar{\imath})$; (ii) we solve the algebraic system (17) for the various eigenvectors which, when multiplied by a suitable amplitude ϵ, represent possible solutions for ϕ; (iii) for each eigenvector, we attempt to find a value ϵ such that $\phi + 2\delta_y j$ is less than unity for every point $j < J(\bar{\imath})$ and greater than unity for all other points. If this final step is completed successfully, we can conclude that the resulting ϕ is a solution of (16) and hence of (15).

When this computation scheme is applied with $\delta_x = \frac{1}{2}$, $\delta_y = \frac{1}{8}$ or $\delta_x = \frac{3}{10}$, $\delta_y = \frac{1}{10}$ and the summation with respect to $\bar{\imath}$ is truncated after 15 or 20 terms, respectively, the size of the algebraic system to be solved ranges upwards, depending on the wave amplitude, from 31 equations for the first case or from 81 equations for the other. Actually, since the lowest mode of motion, to which we are confining our interest, corresponds to the smallest eigenvalue of (17), we may dispense with the time-consuming task of finding a complete solution and use instead the iterative 'power method' (Lapidus 1962) which seeks only the first eigenvalue and the corresponding eigenvector.

With experience it is possible to estimate the shape of the dividing streamline well enough so that a valid solution can be obtained from nearly half the initial guesses. In fact, having assumed the points $J(i)$ and solved the linear equations, it is usually possible to find a range of amplitudes for which all the points with $j < J(i)$, but no others, are included between the dividing streamlines. This uncertainty in wave amplitude is depicted in figure 1, in which the values of λ obtained using the two different mesh sizes and from the approximate three-layer solution are plotted against the dimensionless wave amplitude a, which, for the numerical solutions, is defined as the maximum value of $(y-1)$ along $\psi = 1$. Figures 2 and 3 depict, respectively, the solution for a moderate amplitude and a large-amplitude wave. In plotting these solutions, the value of ϕ was determined at each station $x = x_i$ by linear interpolation in the vertical direction, and the points at which $\psi(x_i, y) =$ constant were then joined by a smooth curve.

It can be seen from the results for the large-amplitude wave that, near the centre of the disturbance, the streamline $\psi = 0$ bifurcates, enclosing a region of

closed streamline flow. This was found to occur for wave amplitudes greater than about 1·2. Unfortunately the present method of analysis ceases to be valid in such regions where the streamlines do not extend to infinity, for, as may be

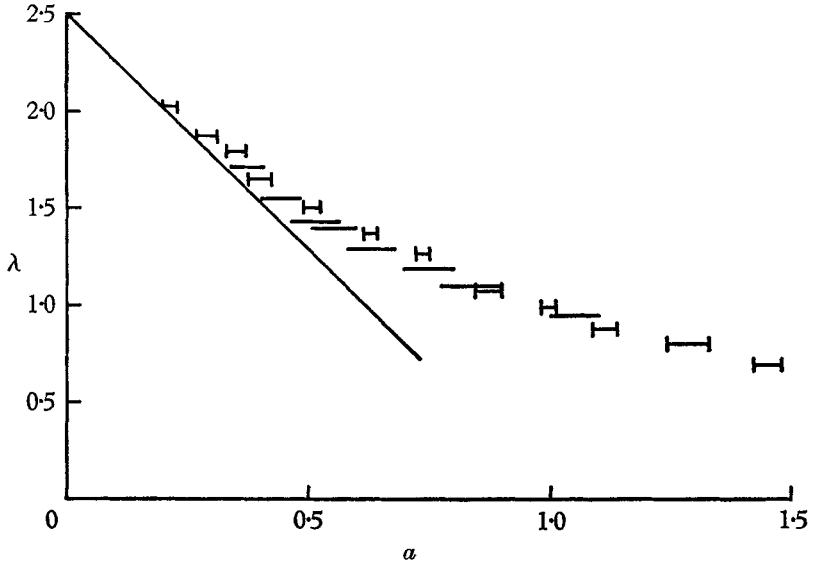

FIGURE 1. The parameter $\frac{1}{2}(gL/U^2)\ln(\rho_2/\rho_1)$ from numerical solutions. ——, coarse mesh; |——|, fine mesh.

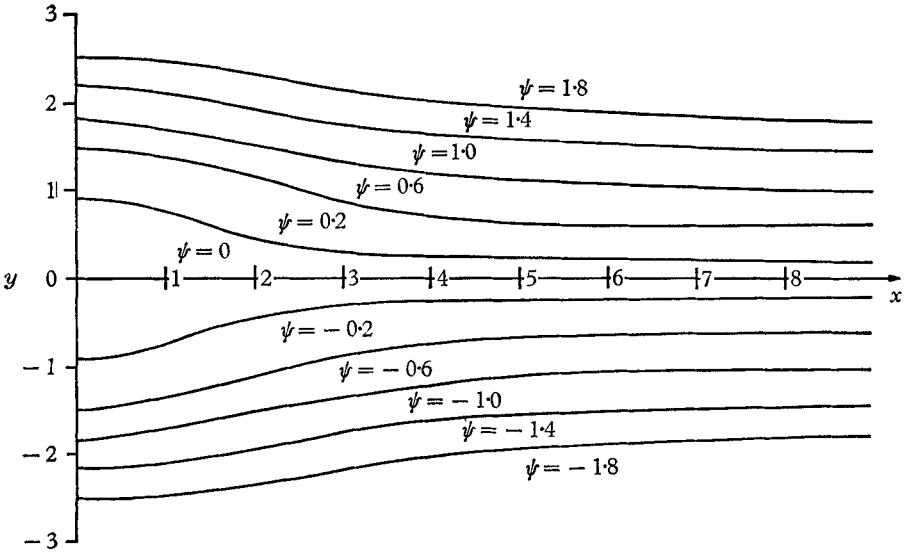

FIGURE 2. Numerical solution for $a = 0{\cdot}8$.

recalled, in arriving at (1), the density $\rho(\psi)$ and the arbitrary function $H(\psi)$ were determined from the known nature of the flow as $x \to \infty$. Although it is true, of course, that one might be able to make a reasonable choice for ρ and H in the closed streamline region of the flow (for example the assumption of uniform

density might be considered acceptable), even so the existence of a closed region in the flow raises a serious question as to the validity of neglecting the effects of viscosity in the analysis. This is so, because, if there are no closed regions we would expect the motion of a fluid with a very small viscosity to differ from the solution of (1) by a small correction which would account for the 'viscous diffusion' of vorticity and the concomitant decrease, with time, of the amplitude

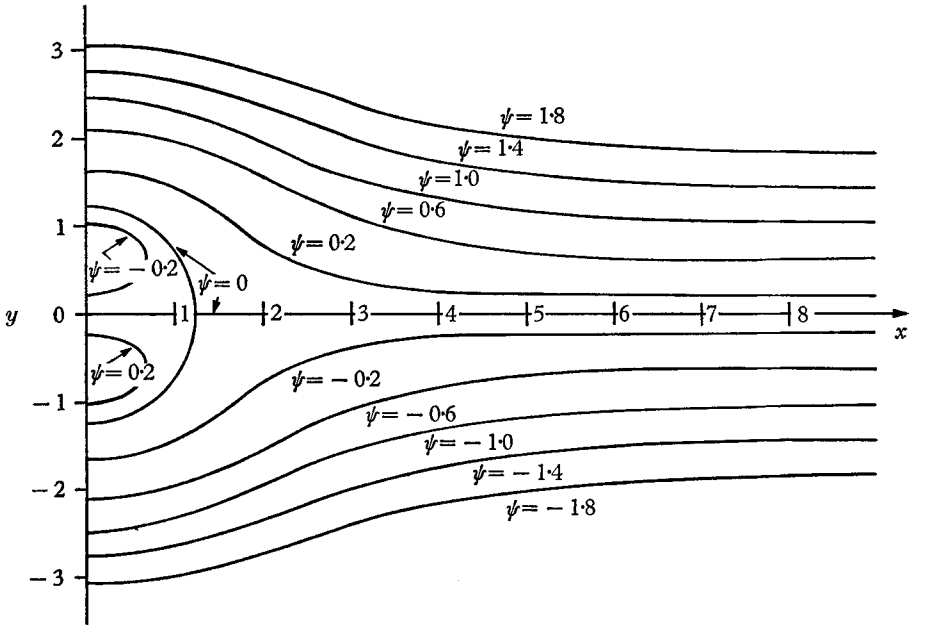

FIGURE 3. Numerical solution for $a = 1{\cdot}4$.

of the wave. On the other hand, as has been pointed out by Batchelor (1956), if there is a region of the flow in which the streamlines are closed, the diffusion of vorticity will have to play an important role in determining the nature of the flow. In particular, since at steady state there is no convection across the boundary of the closed streamline region, the vorticity will have to diffuse throughout its core until it reaches some constant value everywhere. Hence the vorticity in the core cannot be obtained as a state variable of ψ and y, as in (1), but must be determined from knowledge of the flow along the boundary of the closed region, $\psi = 0$.

Owing to the difficulties just discussed, no valid analysis could be found for waves which include regions of closed streamline flow. Nevertheless, the numerical results obtained do present a significant extension of the approximate analytic solutions, particularly in that they indicate the trend of the group λ as the wave amplitude becomes large but still less than about 1·2. The inability to describe waves with closed streamlines is, however, a serious limitation since, as discussed in the following section, waves in this regime can be produced and are, in fact, very effective in promoting mixing across the layer of varying density.

4. Experimental results

The experiments were carried out in a Lucite tank 2·5 m long, 40 cm deep and 10 cm wide which was filled with an appropriately stratified solution of salt and water. The tank was initially half filled with a uniform solution of salt water with a density ranging from 1·17 to 1·05 g/cm^3. Fresh water was then slowly floated on to the salt water, thereby creating two layers of constant density joined by a layer of approximately 1 cm thickness in which the density varied continuously. As the experiments were carried out, the thickness of the gradient layer slowly increased because of diffusion and the mixing associated with the wave generation technique, thus forming a range of density profiles. Drops of a mixture of toluene and carbon tetrachloride coloured with oil red dye, all of which are insoluble in water, were then injected into the upper layer and allowed to settle, thereby demarcating the levels at which they were neutrally buoyant and providing a method for visualizing the flow. The densities of both the salt solutions and the organic mixtures were measured to $\pm 0{\cdot}002$ g/cm^3 by means of a hydrometer.

Perhaps the most remarkable feature of the type of solitary wave under study was the ease with which it could be generated. Almost any disturbance of the density gradient layer would produce a wave of this type, mixed with other wave motions of a transient nature, which, however, could be eliminated by adopting the following technique. A small box was constructed with an open top and a horizontal slit in one side, and was fitted with a plunger with which fluid could be drawn into or ejected from the box through the slit. After the box had been placed at the end of the wave tank with the slit adjusted to the level of the density gradient layer, fluid was drawn into the box and impulsively ejected through the slit. The resulting motion near the slit was quite chaotic, resembling a pulse of turbulent wall jet, but, 20–30 cm farther downstream, the disturbance took the form of a solitary wave and continued to propagate down the tank. Figures 4 and 5, plate 1, are photographs of two such solitary waves, both propagating from left to right between layers of density 1·00 and 1·14 g/cm^3, respectively.

The smaller-amplitude wave in figure 4 is an example of the type of solitary wave modelled by the theoretical analysis of the previous sections. The waveshape, which appears to be asymmetric only because the marker drops were not placed uniformly throughout the density gradient layer, underwent no change, other than a gradual attenuation of amplitude, as the wave propagated down the tank. As would be expected of a wave motion, the fluid velocities associated with this disturbance were less than the propagation velocity. The motion was extremely two-dimensional with no noticeable velocity parallel to the wave front and without significant interaction with the walls of the wave tank. Waves of this type were found to reflect off the end of the tank without losing much of their energy and two waves travelling in opposite directions would pass through each other and travel on without further change of shape.

In contrast, the wave depicted in figure 5, although of only slightly greater amplitude than that shown in figure 4, had a character entirely different from that treated in the theoretical analysis. In such waves the waveshape was not steady and semiperiodic waves were seen being shed behind the main disturb-

ance. In addition, the fluid velocity at the centre of the wave was found to be approximately equal to the propagation velocity, giving to the motion the appearance of a 'lump' of fluid moving through the region of varying density. In fact, regions of closed streamline flow, quite similar to those seen in the large-amplitude numerical solutions, were often observed. However, as viscous dissipation and the unsteady semiperiodic waves extract energy from the main motion, such lumps decayed to small-amplitude waves of the type pictured in figure 4.

In addition to such qualitative observations of the wave behaviour, the experimental programme included the measurement of wave propagation velocities. While neither of the idealized density profiles used for the analysis could be duplicated exactly, the actual density profile was found to be approximately of the form $\ln\rho = (d\ln\rho/d\psi)_{\max}\tanh y/L + C$ which was used in developing the inner and outer solution. Therefore, in order to compare measured wave speeds to the predictions of our theoretical model, we chose to treat our data by assuming that the density variation was of this form.

The constant $(d\ln\rho/d\psi)_{\max}$ is given simply as $\frac{1}{2}\ln(\rho_1/\rho_2)$, where ρ_1 and ρ_2 are, respectively, the densities of the upper and lower homogeneous layers. The characteristic length L was determined by measuring the elevation of various neutrally buoyant drops of known density and fitting the data to the assumed function, $\tanh(y/L)$, and the propagation velocity was found by timing the passage of a wave through a measured meter. It was then possible to compute the group $\lambda = -(gL/U^2)(d\ln\rho/d\psi)_{\max}$ which is the fundamental parameter of our analysis.

From photographs similar to figures 4 and 5, which were taken as the wave passed through the measured meter, it is possible to determine the value of ϕ along those lines of constant density which are demarcated by neutrally buoyant drops. Unfortunately, the amplitude parameter ϵ, used in the analysis, is defined only in terms of the expansion $\phi = \epsilon\phi^{(1)} + \epsilon^2\phi^{(2)} + \ldots$ and hence cannot be determined without knowledge of the complete analytic solution. We have chosen, therefore, to express our results in terms of the amplitude parameter a defined by

$$a = -\phi_{\text{ext}}(\rho)\,\frac{\ln\rho(\rho_1\rho_2)^{-\frac{1}{2}}}{\ln(\rho_1/\rho_2)^{\frac{1}{2}}}, \tag{18}$$

where ρ_1 and ρ_2 are the densities of the upper and lower layers, respectively, and ϕ_{ext} is the extremum value of ϕ along the line of constant density ρ. This amplitude parameter is closely related to ϵ, being, in fact, the value of ϵ computed from the first-order analysis for which

$$\phi_{\text{ext}} = \epsilon\phi^{(1)}|_{x=0}, \quad \ln\rho(\rho_1\rho_2)^{-\frac{1}{2}} = \ln(\rho_1/\rho_2)\tanh y.$$

In principle, since the dependence of ϕ_{ext} and $\phi^{(1)}$ on ρ are not exactly the same, we would expect the amplitude a to depend on ρ. But in practice it was found that a as computed from ϕ_{ext} for different lines of constant density was essentially independent of ρ.

The results of measurements of waves propagating between layers of fresh water and salt solutions having densities of 1·052, 1·095 and 1·168 g/m³. are presented in figure 6, in which measured values of λ are seen plotted against the

amplitude parameter a. The analysis predicts that as a becomes small λ should equal $2{\cdot}0-1{\cdot}2\epsilon$ or, since $a = \epsilon + O(\epsilon^2)$, that $\lambda = 2{\cdot}0 - 1{\cdot}2a$. The close agreement between the experimentally determined values of λ and this expression serves as a remarkable corroboration of the linearized theory based on the long wave

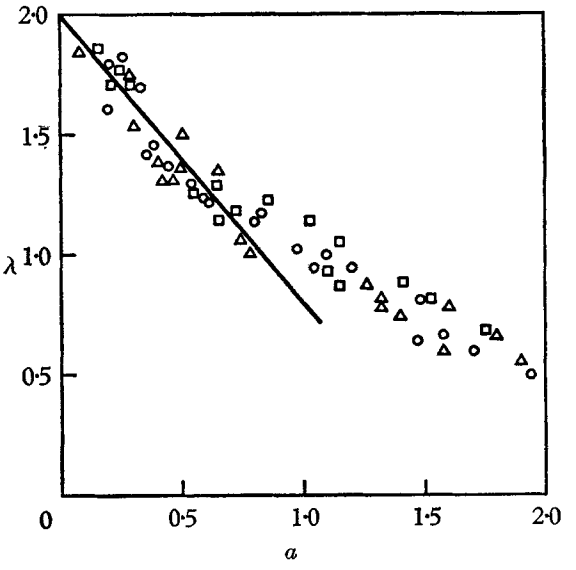

FIGURE 6. The parameter $\frac{1}{2}(gL/U^2)\ln(\rho_2/\rho_1)$; $\rho_1 = 1{\cdot}000$ g/cm^3, △, $\rho_2 = 1{\cdot}052$; □, $\rho_2 = 1{\cdot}095$; ○, $\rho_2 = 1{\cdot}168$.

assumption. Comparing figure 6 to figure 1, in which the value of λ obtained from the numerical solutions for a three-layer fluid are presented, we are also led to conclude that the deviation from the linear theory is a finite-amplitude effect which could be accounted for by considering terms of higher order in ϵ. It would appear, then, that neither the viscosity nor the finite depth of the water (in dimensionless distance always greater than 40) had a significant influence on the propagation velocity and that the idealized density profile assumed in the analysis was adequate to describe the configuration actually encountered.

This work was supported in part by a grant from the Office of Saline Water and by a National Science Foundation fellowship to Russ E. Davis.

REFERENCES

BATCHELOR, G. K. 1956 On steady laminar flow with closed streamlines at large Reynolds number. *J. Fluid Mech.* **1**, 177.

BENJAMIN, T. B. 1966 Internal waves of finite amplitude and permanent form. *J. Fluid Mech.* **25**, 241.

BENJAMIN, T. B. 1967 *J. Fluid Mech.* **29**, 559.

COURANT, R. & HILBERT, P. 1953 *Methods of Mathematical Physics*, I. New York: Interscience.

LAPIDUS, L. 1962 *Digital Computation for Chemical Engineers*. New York: McGraw-Hill.

LONG, R. R. 1953 Some aspects of the flow of stratified fluids. I. A theoretical investigation. *Tellus* **5**, 42.

LONG, R. R. 1965 On the Boussinesq approximation and its role in the theory of internal waves. *Tellus* **17**, 46.

PETTERSSON, O. 1912 Climatic variations in historic and prehistoric time. *Svenska Hydrog-Biol. Kromm. Skrifter* **5**.

YIH, C. S. 1960*a* Gravity waves in a stratified fluid. *J. Fluid Mech.* **8**, 481.

YIH, C. S. 1960*b* Exact solutions for steady two-dimensional flow of a stratified fluid. *J. Fluid Mech.* **9**, 161.

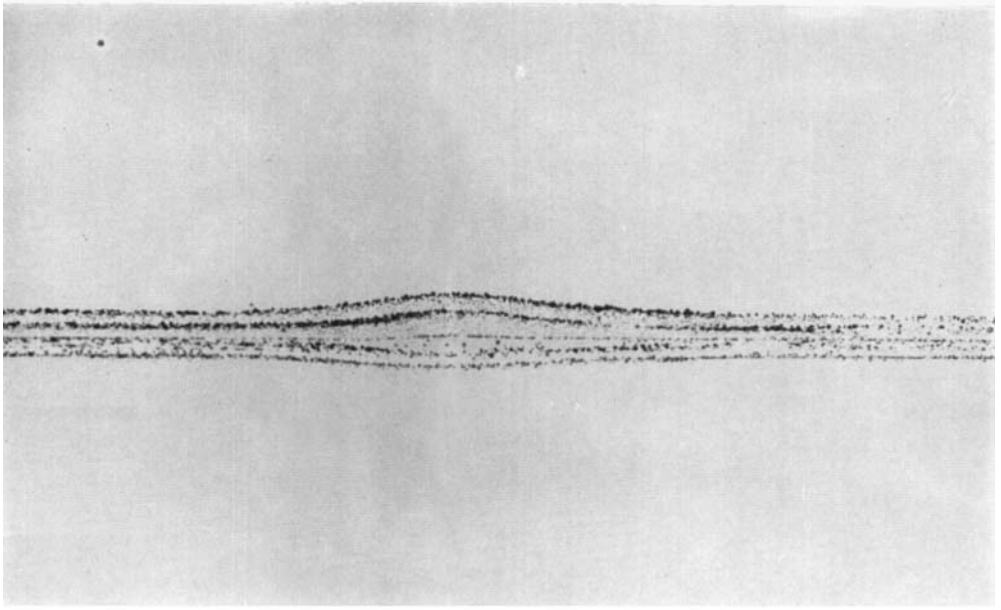

FIGURE 4.

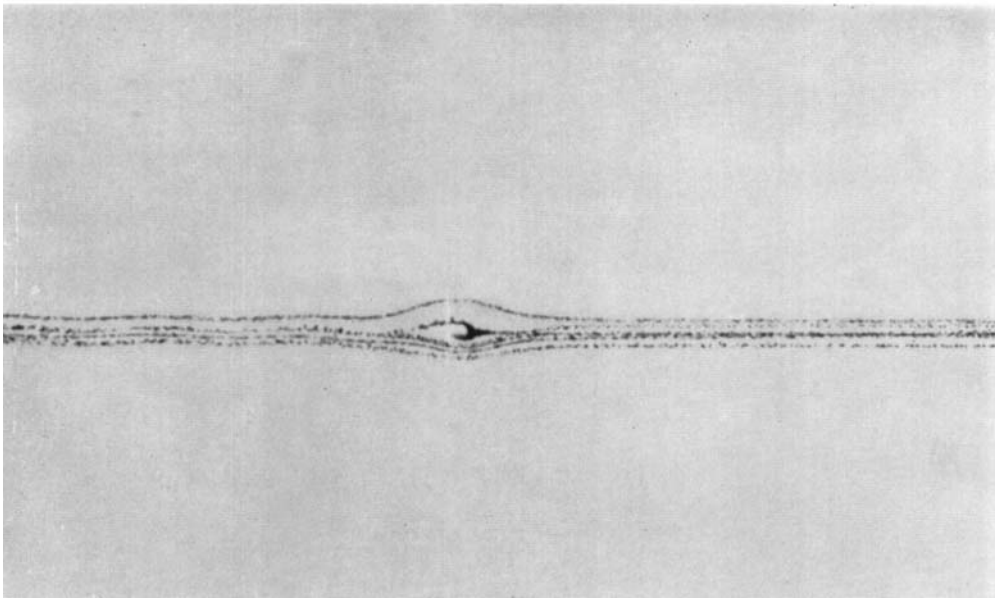

FIGURE 5.